2000

Asymmetry and rectification in the tunnel current of a nanometer-sized metal-conjugated polymer-metal junction

S T. Yau
University of Wollongong

C Zhang
University of Wollongong, czhang@uow.edu.au

Peter Innis
University of Wollongong, innis@uow.edu.au

Asymmetry and rectification in the tunnel current of a nanometer-sized metal-conjugated polymer-metal junction

Abstract

Electron transport processes of a nanometer metal-conjugated polymer–metal tunnel junction have been probed using a scanning tunneling microscope. The tunnel current of the junction shows two effects. The appearance of an asymmetry in the tunnel current indicates that the junction transport mechanism is different from that for which tunneling occurs directly between two metallic electrodes. Thus, understanding of the asymmetry and hence the transport mechanism demands a detailed description of the metal–polymer interface. By applying the theories of the metal–semiconductor interface to the tunnel junction, we show the presence of an asymmetric electrostatic potential-energy profile, which, together with the metal-induced gap states in the polymer, gives rise to the observed asymmetry in the tunnel current. In some cases, a threshold of anomalously large currents enhances the current asymmetry to give rise to rectification, indicating carrier excitations and carrier multiplication processes in the junction. Our results show that a detailed description of the interface electronic structure is essential to understanding electron transport in devices based on organic molecules.

Keywords

conjugated, junction, asymmetry, current, tunnel, polymer, metal, sized, nanometer, rectification

Disciplines

Engineering | Physical Sciences and Mathematics

Publication Details

Yau, S. T., Zhang, C. & Innis, P. C. (2000). Asymmetry and rectification in the tunnel current of a nanometer-sized metal-conjugated polymer-metal junction. Journal of Chemical Physics, 112 (15), 6774-6778.

Asymmetry and rectification in the tunnel current of a nanometer-sized metal-conjugated polymer–metal junction

S.-T. Yau, C. Zhang, and P. C. Innis

Citation: The Journal of Chemical Physics **112**, 6774 (2000); doi: 10.1063/1.481252
View online: http://dx.doi.org/10.1063/1.481252
View Table of Contents: http://scitation.aip.org/content/aip/journal/jcp/112/15?ver=pdfcov
Published by the AIP Publishing

Asymmetry and rectification in the tunnel current of a nanometer-sized metal-conjugated polymer–metal junction

S.-T. Yau[a)]
Department of Materials Engineering, University of Wollongong, NSW 2522, Australia

C. Zhang
Department of Engineering Physics and Institute for Superconducting and Electronic Materials, University of Wollongong, NSW 2522, Australia

P. C. Innis
Intelligent Polymer Research Institute, University of Wollongong, NSW 2522, Australia

(Received 12 November 1999; accepted 21 January 2000)

Electron transport processes of a nanometer metal-conjugated polymer–metal tunnel junction have been probed using a scanning tunneling microscope. The tunnel current of the junction shows two effects. The appearance of an asymmetry in the tunnel current indicates that the junction transport mechanism is different from that for which tunneling occurs directly between two metallic electrodes. Thus, understanding of the asymmetry and hence the transport mechanism demands a detailed description of the metal–polymer interface. By applying the theories of the metal–semiconductor interface to the tunnel junction, we show the presence of an asymmetric electrostatic potential-energy profile, which, together with the metal-induced gap states in the polymer, gives rise to the observed asymmetry in the tunnel current. In some cases, a threshold of anomalously large currents enhances the current asymmetry to give rise to rectification, indicating carrier excitations and carrier multiplication processes in the junction. Our results show that a detailed description of the interface electronic structure is essential to understanding electron transport in devices based on organic molecules. © *2000 American Institute of Physics.* [S0021-9606(00)70215-7]

Present technology has indicated that nanometer-sized devices (nanodevice) can be fabricated by manipulating single nanometer-sized particles (nanoparticle) such as organic and biological molecules[1–3] and inorganic clusters.[4–7] In many cases, single nanoparticles perform specific functions. The electron transport properties of single nanoparticles, the functional ''building blocks,'' have to be understood in order to realize nanodevices. To date, single-electron tunneling (SET) has been observed with thermally evaporated metal particles at low temperatures[8,9] and at room temperature[10,11] using the scanning tunneling microscope (STM). Recently, the STM has been used to obtain SET signals at room temperature from individual insulator-coated gold colloid particles.[12] Organic molecules also show interesting transport phenomena.[13,14] Specifically designed organic molecules consisted of an electron donor and an electron acceptor, which are connected to each other by a σ-bridge, give rise to current rectification.[15,16] This kind of molecule is of prime importance in molecular electronics. Conjugated polymers (CP) chains with overlapping π-electron wave functions have been proposed to be used in information storage devices.[17] The one-dimensional (1D) nature of CP provides strong localization of electrons so that high storage capacity can be achieved. In general, a thorough understanding of electron transport properties of a nanometer-sized CP–metal junction demands a detailed description of the metal–CP interfacial electronic structures.

In this paper, we report a study on the electron transport mechanisms of a nanometer-sized metal–CP–metal tunnel junction. We also present a detailed description of the metal–CP interfacial electronic structure, which is essential to understanding the transport mechanisms. We have observed two effects in the tunnel current of the junction, that was composed of a single CP nanoparticle sandwiched between two metallic electrodes. An asymmetry in the tunnel current indicates that the junction transport mechanism is different from that for which tunneling occurs directly between two metallic electrodes. In some cases, a threshold of anomalously large currents enhances the current asymmetry to give rise to rectification, indicating carrier excitations and carrier multiplication processes in the junction. We have applied theories of the metal–semiconductor interface to the metal–CP interface. Detailed analysis of the electronic structures of the junction shows an asymmetric electrostatic potential energy profile, which, together with the metal-induced gap states in the polymer, causes the two interfacial regions to have asymmetry electron concentrations separated by a potential barrier. Under a bias, an asymmetry in the tunnel current appears as observed experimentally. This asymmetric potential-energy profile also leads to an asymmetric distribution of electric fields near the two interfacial regions, where impact ionization can be induced to enhance the current asymmetry resulting in rectification.

The CP particles used in this experiment were colloidal

a)Author to whom correspondence should be addressed. Present address: CMMR, RI Building D-29, University of Alabama at Huntsville, Huntsville, AL, 35899; Electronic mail: vaust@email.uah.edu

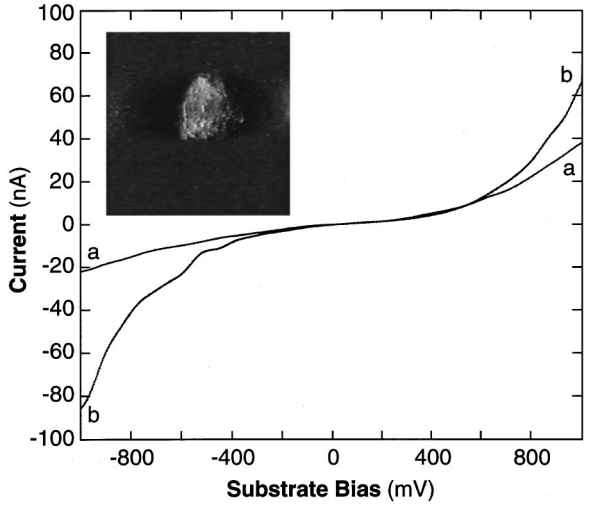

FIG. 1. Curve a was taken near the center of the EB particle shown in the inset. Curve b is the reference taken on the HOGP substrate. Both curves were obtained under the same biasing conditions. The inset is a STM image (50 nm×50 nm) of an EB particle.

emeraldine base (EB), which is the semiconducting form of the polyaniline (PANI). Polystyrene sulfonate (PSS) was used as the steric stabilizer. PANI/PSS colloid synthesis was performed in a divided electrochemical flow-through cell.[18] The anode and cathode were fabricated from porous reticulated vitreous carbon (RVC), with a porosity of 100 pores per inch (PPI) and an effective surface area of 65.6 cm^2/cm^3 (ERG Materials and Aerospace Corp.). Two cathode disks (20×50 mm, 2576 cm^2) were employed on the opposite faces of the anode (15×50 mm, 1932 cm^2) to give uniform electric field distribution. The anode RVC disk was separated from the two cathodes by an ion exchange membrane (Neosepta AMH A-2119, Tokuyama Corp.) to prevent mixing of the anode and cathode solutions. An anode synthesis solution (500 mL) was prepared containing 0.25 mol/L $H_2SO_4(aq)$, 0.1 mol/L aniline, and 3 g/L PSS (1.5 g), together with a separate cathode solution (500 mL) containing 0.5 mol/L $NaNO_3(aq)$. These electrolyte solutions were passed through their respective compartments at a flow rate of 165 mL/min by peristatic pump. Electropolymerization was carried out at +0.90 V vs Ag–AgCl for a total of 2.5 h to form an emeraldine salt (ES) dispersion. The colloidal ES dispersion was then dialyzed for 24 h using cellulose membrane dialysis tubing with a molecular weight cutoff greater than 12 000 Daltons (Sigma) to remove excess aniline monomer and H_2SO_4. To this solution, excess NaOH was added to convert the ES to EB. The solution was then redialyzed.

To form the tunnel junction, whose electron transport mechanisms were to be studied, the PtIr scanning tip of a STM was positioned above an individual EB particle, which was deposited in a drop of the colloid suspension on a highly oriented pyrolytic graphite (HOPG) surface. The inset in Fig. 1 shows a STM image of an EB particle. The 16 nm particle has a circular shape with chainlike structures covering its surface. These 1.2 nm wide chains are the PSS coating on the particle surface. It was found that the chains can be ''pushed'' to the sides of a particle by the scanning action of the tip to expose the crystalline structures of the EB particle.[19] The average height of the EB particle is 14 nm and the variation of the height across the particle surface is 2.5 nm. Current-voltage ($I-V$) curves of the particle were taken under ambient conditions. Each point on a curve is the average of ten current values corresponding to the same bias voltage. $I-V$ curves were taken at different locations on the particle. The curves were reproducible at each location. $I-V$ curves were also taken on the HOPG substrate as the reference, that is to be compared to the particle $I-V$ curves. Since the HOPG surface is chemically inert, the particles were only physically attached to the surface. Some particles had stronger attachment than others. It was observed that large biases tend to move the particles, making measurement difficult. Therefore, we selected firmly attached particles by the observation that they did not move during measurement and we had to keep the bias between +1 V and −1 V.

An asymmetry in the tunnel current is reflected in the $I-V$ curves of the junction. Figure 1 shows two $I-V$ curves: Curve a was taken at the center of the particle shown in the inset, and curve b, the reference, was taken on the HOPG substrate 20 nm away from the particle. Curve b is asymmetric with the current increases faster in the negative substrate bias polarity as reported previously.[20] This asymmetry is due to the difference in the workfunctions of the substrate and the tip, which results in an offset in the conductance minimum.[21] On the contrary, curve a increases faster in the positive substrate polarity. In both polarities, the current level of curve a is below that of curve b. Therefore, the asymmetry of curve a and its reversal in the polarities differentiate the electron transport process in the metal–CP–metal junction from the direct tunneling between the tip and the HOPG substrate. Another interesting feature of curve a is that the band-gap of EB is not reflected in the $I-V$ curve, since, for a semiconductor, there should be a flat region in the $I-V$ curve where the current is extremely small. Such a gap has been observed with EB films.[22]

To understand the origin of the observed asymmetry in the tunnel current, it is necessary to construct the energy-band diagram of the tunnel junction together with a detailed description of the metal–CP interface such as the schematic presentations (not drawn to scale) in Fig. 2. Recently, we have revealed the crystalline structure of nanometer EB colloid particles using the STM.[19] Our result shows that the EB particle has the same crystalline structure as bulk EB. Thus, we can apply the calculated energy-band structure of bulk EB[23] to the particles as shown in Fig. 2(a). EB is an intrinsic semiconductor, whose band structure in the band-gap region is characterized by a 1.2 eV gap separating the conduction band, E_C, and the valence band, E_V, which have very weak dispersion.[24] The Fermi energy, E_F, is located half way between E_V and E_C. The first empty band above E_C, denoted by E_H, is dispersionless and is separated from E_C by a gap of 3.2 eV. In Fig. 2(a), E_l and E_r denote the energy of E_C below E_F at the left and right interfaces, respectively. The calculated energy-band diagram of bulk EB[24] shows that the work function and the electron affinity of EB are 6.2 and 5.8 eV, respectively. The work functions of PtIr[25] and HOPG[26] are 5.6 and 5.0 eV, respectively. Using these data, E_l and E_r

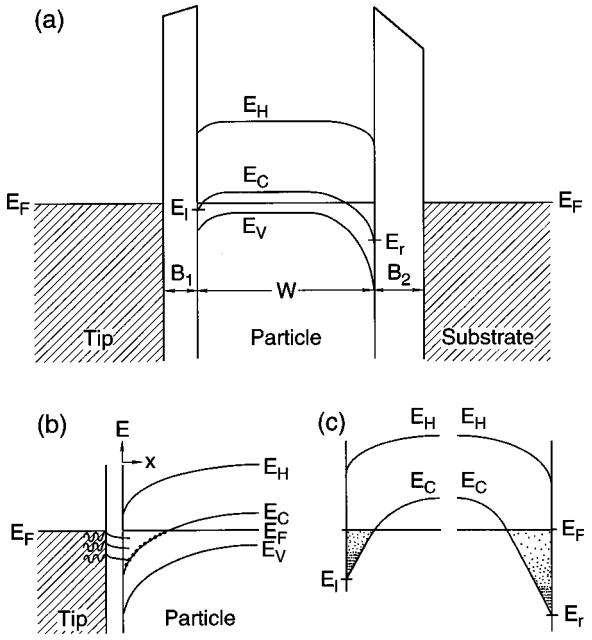

FIG. 2. (a) Schematic energy-band diagram of the tunnel junction. The conduction band, the valence band, and the first band above the conduction band are represented by E_C, E_V, and E_H, respectively. The widths of the left (tip-particle) barrier and the right (particle-substrate) barrier are presented by B_1 and B_2, respectively. W is the particle width. E_F denotes the Fermi energy. E_l and E_r are the values of E_C relative to E_F at the left and right interfaces, respectively. The tip and the substrate are represented by two simple metals. (b) A detailed schematic energy-band diagram of the left interface at zero-bias. The black dots represent electrons occupying the states of E_C. The wave functions of the evanescent states of the metal are shown to indicate the presence of the MIGS. (c) A schematic description of the electron distributions near the two interfaces.

are calculated to be -0.2 and -0.8 eV, respectively. We will show that this asymmetry in the electrostatic potential-energy profile gives rise to the observed asymmetry in the tunnel current when a bias is applied between the two electrodes, that are represented by two simple metals. B_1 is the width of the barrier belonging to the left interface, which is air between the tip and the EB surface as explained above. B_1 is $\sim$5 A. B_2, $\sim$10 A, is the width of the right barrier, that is composed of the PSS coating. The average thickness of the EB particle, W, is estimated to be 14 nm. Our calculation of the screening length of emeraldine base is based on the fact that there is 2×10^{-3} polaron per benzenoid ring, and the volume of a ring is $125\times10^{-24}\,\mathrm{cm}^3$.[27] These lead to a density of carrier of $1.6\times10^{19}\,\mathrm{cm}^3$, resulting in a screening length of 1 nm. To show the mechanism of the transfer of electrons across the tunnel junction and hence the origin of the asymmetry in tunnel current, it is necessary to invoke the theory of metal-induced gap states (MIGS).[28,29] At the interface between a metal and a semiconductor, the Bloch states of the metal leak into the band gap of the semiconductor as evanescent states. Matching states at the interface results in a continuous distribution of density of state in the band gap, $\rho(E)$, that has a minimum near the middle of the band gap and diverges near E_C and E_V.

Figure 2(b) shows a detailed schematic energy-band structure of the left interface at zero-bias. The states on E_C below E_F are occupied by electrons that tunneled from the metal when the junction was formed in order to achieve thermal equilibrium. These electrons do not contribute to the current asymmetry, since the density of states on E_C is a constant. Due to the fact that E_C has very weak dispersion, the region between the interface boundary ($x=0$) and E_C should not contain states. However, in this region, the occupied E_C is separated by the 3.2 eV gap from E_H. Thus, this region resembles the interface between a metal and a semiconductor with E_C functions as the valence band and E_H as the conduction band. Therefore, MIGS are induced in this region with a distribution of $\rho(E)$. Assuming a 1D problem and denoting $\phi(x)$ as the wave functions of the evanescent states of the metal having the form of $e^{-qx}\sin(kx)$, the electron concentration at an energy E above E_C is $n(x,E)=|\phi(x)|^2\rho(E)$. Therefore, along the trajectory of a constant value of $\rho(E)$ parallel to E_C below E_F, a point located closer to the interface boundary will have a larger $n(x,E)$ than the points that are located further away due to q, the decaying factor of ϕ. Therefore, when the junction was formed, electrons from the tip populated the MIGS in the region of the left interface, and electrons from the substrate populated the MIGS in the region of the right interface. Figure 2(c) shows schematically the electron distribution in the two interfacial regions.

Assume the decay lengths of the evanescent states near the two interfaces are the same and are represented by t. Because $n(x,E)$ is higher close to the interface for a constant E and $\rho(E)$ is higher when the electron energy is close to E_C, the average energy of electron occupying the MIGS near the left interface is higher than those near the right interface. To simplify the discussion, we assume that the band profile near the left interface is linear in x, x being the distance measured from the interface. Therefore, the energy profile which is at a constant but infinitesimal amount of energy above E_C, is expressed by

$$E_{C,L}=E_l+\alpha x \tag{1}$$

where, $E_l=-0.2$ eV, and α is a constant. A similar expression $E_{C,R}$ can be written for the region near the right interface. At equilibrium, the average energy of electrons occupying the left and the right MIGS can be approximately given as

$$\langle E^L_{\mathrm{MIGS}}\rangle\approx\left|\phi\left(\frac{t}{2}\right)\right|^2\left(E_l+\alpha\frac{t}{2}\right) \tag{2}$$

and

$$\langle E^R_{\mathrm{MIGS}}\rangle\approx\left|\phi\left(\frac{t}{2}\right)\right|^2\left(E_r+\alpha\frac{t}{2}\right), \tag{3}$$

respectively.

Since $E_l=-0.2$ eV and $E_r=-0.8$ eV, $\langle E^L_{\mathrm{MIGS}}\rangle$ is several hundreds meV higher than $\langle E^R_{\mathrm{MIGS}}\rangle$. This asymmetric average electron energy is the origin of the observed asymmetry in the $I-V$ curves. When a positive substrate bias is applied, electrons in the left MIGS tunnel across the central barrier setup by the middle portion of E_C to the substrate. The process can be regarded as resonant tunneling via resonant states, which are those empty MIGS at the right interface created by the bias. The same tunneling process can also occur under a negative substrate bias. Since $\rho(E)$ of the MIGS diverges close to E_C and ϕ is large close to the inter-

face, therefore, for a given magnitude of bias, there will be more electrons tunneling through the barrier when the substrate bias is in the positive polarity [see Fig. 2(c)]. As a result, the $I-V$ curves exhibit an asymmetry.

The relative strength of the tunneling currents of the two bias polarities can be estimated. To simplify the analysis, we shall consider only the electrons that populate $\rho(E)$ very close to E_C, i.e., the tunneling electrons have energy $E_{C,L}$ and $E_{C,R}$. Under a positive substrate bias, the current can be written as

$$j_L = \int dE \rho(E) n_L(E) T(E) [f_L(E) - f_R(E + \mathrm{eV})], \qquad (4)$$

where $T(E)$ is the tunneling rate, $n(E)$ is the energy dependent electron concentration, $f(E)$ is the Fermi distribution function, and V is the bias. The electron concentration can be expressed as

$$n_L(x) = |\phi(x)|^2 \propto \exp(-2qx) = \exp\left[-2q \frac{(E_{C,L} - E_1)}{\alpha}\right] = n_L(E). \qquad (5)$$

The parameter α decreases with the bias, i.e., $\alpha \rightarrow \alpha - \beta V$. When the bias polarity is reversed

$$j_R = \int dE \rho(E) n_R(E) T(E) [f_R(E) - f_L(E + \mathrm{eV})]. \qquad (6)$$

However, in this case $n_R(E)$ is smaller, i.e.

$$n_R(E) = \exp\left[-2q \frac{(E_{C,R} - E_r)}{\alpha}\right] = \exp\left[-2q \frac{(E_{C,R} - E_l + \Delta E)}{\alpha}\right], \qquad (7)$$

where $\Delta E = 0.6\,\mathrm{eV}$. Therefore, $n_R(E)$ is smaller compared to $n_L(E)$ by a factor of $\exp(-q\Delta E/\alpha)$. Since α is bias dependent, we obtain

$$r = \frac{j_L}{j_R} \approx \exp\left[2q \frac{\Delta E}{\alpha - \beta V}\right]. \qquad (8)$$

Thus, the ratio of the current under a positive sample bias to that under a negative sample bias is greater than unity and is an increasing function of the bias. This is in agreement with the experimental results.

As shown in Fig. 1, due to the larger tip-substrate separation [see Fig. 2(a)], the current level of the tunnel junction is less than that of the reference current due to electron tunneling between the tip and the HOPG substrate. However, in thin regions such as the regions close to the right edge of the particle in Fig. 1, the $I-V$ curves show a threshold in the positive substrate bias polarity, after which the current level begins to exceed the reference resulting in rectification of the tunnel current. For the curve in Fig. 3, the threshold occurs at ~800 meV. We believe that the anomalously large currents are due to impact ionization, which modifies the transport mechanism responsible for the current asymmetry described earlier. The asymmetric potential-energy profile of the junction again plays a key role in this regard. Figure 2(a) shows that the potential-energy profile of the particle near the right

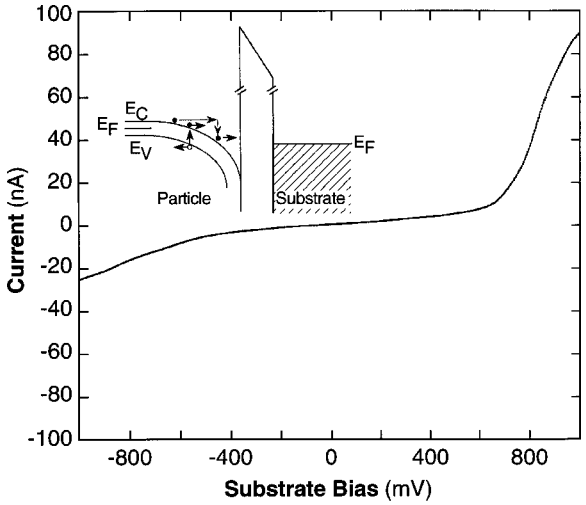

FIG. 3. An $I-V$ curve taken at a location close to the right edge of the particle in Fig. 1 exhibiting current rectification. The curve was obtained under the same biasing conditions as those in Fig. 1. The inset shows a schematic energy-band diagram of the right interface under a positive substrate bias. The process of impact ionization is depicted with electrons and holes presented by black and open circles, respectively.

interface decreases more rapidly than that near the left interface. This indicates that the electric field within the particle is larger in the region close to the right interface. The inset of Fig. 3 shows that, as a positive sample bias is applied, the field close to the right interface increases to accelerate electrons in E_C of the particle to kinetic energies above E_C. These electrons are no longer in thermal equilibrium with the lattice. If the energy of these hot electrons is large enough, electron-hole pairs will be generated when the hot electrons collide with the valence electrons giving up their excess energy. This is the process of impact ionization. For the negative sample bias polarity, impact ionization requires larger biases so that the field near the left interface is large enough to reach the ionization threshold. If we assume that the effective masses for E_V and E_C are the same, impact ionization will occur when the energy of the field-accelerated electrons, E_i, exceeds $E_{\min} = 1.5\,E_G$,[30] where E_G is the band-gap. The amount of band-bending at the right interface is 1.4 eV at zero-bias. As the positive substrate bias increases, the band-bending also increases. If half of the bias drops on the right portion of E_C, the band-bending will reach 1.8 eV ($=1.5E_G$) when the bias exceeds 800 meV. Therefore, one expects the onset of impact ionization to occur at 800 meV. This is in good agreement with the experimental observation as shown in Fig. 3. Beyond this threshold, a term proportional to $\exp[-2(E_i/\mathrm{eV})]$ will contribute to the current leading to avalanche breakdown, and thus rectification occurs. Note that secondary carrier generation due to relaxation of hot electrons has also been observed in other nanoparticles.[12]

From the above discussion, it is obvious that the size of the particles, W, is also important in the electron transport process. If W is too large, quantum-mechanical tunneling across the particle will be weak, and, in the case of impact ionization, some of the secondary carriers may not be able to reach the right interface to tunnel to the substrate. These effects have been observed in the experiment as described

above. Thus, nanoparticles are suitable for the observation of the transport phenomena.

[1] T. A. Jung, R. R. Schlittler, J. K. Gimzewski, H. Tang, and C. Joachim, Science **271**, 181 (1996).
[2] M. T. Cuberes, R. R. Schlittler, and J. K. Gimzewski, Appl. Phys. Lett. **69**, 3016 (1996).
[3] S.-T. Yau and Y. Zhou, Mod. Phys. Lett. B **9**, 187 (1995).
[4] A. P. Alivisatos, K. P. Johnson, X. Peng, T. E. Wilson, C. J. Loweth, M. P. Bruchez, and P. G. Schultz, Nature (London) **382**, 609 (1996).
[5] C. A. Mirkin, R. L. Letsinger, R. C. Mucic, and J. J. Storhoff, Nature (London) **382**, 607 (1996).
[6] A. van Blaaderen, R. Ruel, and P. Wiltzius, Nature (London) **385**, 321 (1997).
[7] C. Baur, B. C. Gazen, B. E. Koel, T. R. Ramachandran, A. A. G. Requicha, and L. Zini, J. Vac. Sci. Technol. B **15**, 1577 (1997).
[8] R. Wilkins, E. Ben-Jacob, and R. C. Jacklecic, Phys. Rev. Lett. **63**, 801 (1989).
[9] J.-C. Wan *et al.*, Phys. Rev. B **42**, 5604 (1990).
[10] C. Schonenberger, H. van Houten, and H. C. Donkersloot, Europhys. Lett. **20**, 249 (1992).
[11] R. P. Andres, T. Bein, M. Dorogi, S. Feng, J. Henderson, C. Kubiak, W. Mahoney, R. Osifchin, and R. Reifenberger, Science **272**, 1323 (1996).
[12] S.-T. Yau, P. Mulvaney, W. Xu, and G. Spinks, Phys. Rev. B **57**, R15124 (1998).
[13] S. Datta, W. Tian, S. Hong, R. Reifenberger, J. I. Henderson, and C. P. Kubiak, Phys. Rev. Lett. **79**, 2530 (1997).
[14] M. A. Reed *et al.*, Science **278**, 252 (1997).
[15] A. Aviram and M. A. Ratner, Chem. Phys. Lett. **29**, 277 (1974).
[16] A. S. Martin, J. R. Sambles, and G. J. Ashwell, Phys. Rev. Lett. **70**, 218 (1993).
[17] F. L. Carter, in *Molecular Electronic Devices*, edited by F. L. Carter (Marcel Dekker, New York and Basel, 1982), p. 51.
[18] J. N. Barisci *et al.*, Synth. Met. **84**, 181 (1997); P. C. Innis *et al.*, in *Antec 98*, 1224 (1998).
[19] S.-T. Yau and P. Innis, unpublished.
[20] Curve b shows the ''generic'' feature of the $I-V$ curve of the HOPG substrate probed with a metallic tip, that has been observed in other publications. [M. Kuwabara *et al.*, Appl. Phys. Lett. **56**, 2396 (1990); M. Pomerantz *et al.*, Science **255**, 1115 (1992); C. L. Claypool *et al.*, J. Phys. Chem. B **101**, 5978 (1997)].
[21] J. M. Rowell, in *Tunneling Phenomena in Solids*, edited by E. Burstein and S. Lundqvist (Plenum, New York 1969), pp. 385–404.
[22] S.-T. Yau, J. N. Barisci, and G. Spinks, Appl. Phys. Lett. **74**, 670 (1999).
[23] The band structure of tetramers of EB has been calculated. [S. Stafstrom, in *Electronic Properties of Conjugated Polymers*, edited by H. Kuzmany, M. Mehring, and S Roth (Springer-Verlag, 1987); C. B. Duke, E. M. Conwell, and A. Paton, Chem. Phys. Lett. **131**, 82 (1986)]. It is in good agreement with experimental observation and with the polymer (bulk EB) equivalent. The length of the unit cell of EB is 2 nm. The size of the EB particle is about 14 nm. Thus, we can assume that the band structure of the particle is the same as that of the bulk EB. Also, for the size of the particle, quantum-size effect will not be observed at room temperature. [R. Kubo, J. Phys. Soc. Jpn. **17**, 975 (1962)].
[24] D. S. Boudreaux *et al.*, J. Chem. Phys. **85**, 4584 (1986).
[25] G. A. Haas and R. E. Thomas, in *Techniques of Metals Research*, edited by E. Passaglia (Interscience, New York, 1972), Vol. 6, p. 91.
[26] B. Robrieux, R. Faure, and J. P. Dussaulcy, C. R. Seances Acad. Sci., Ser. B **278**, 659 (1974).
[27] F. Fou, M. Angelopoulos, A. G. MacDiarmid, and A. J. Epstein, Phys. Rev. B **39**, 3570 (1989).
[28] V. Hiene, Phys. Rev. **138**, 1689 (1965).
[29] J. Tersoff, Phys. Rev. Lett. **52**, 465 (1984).
[30] K. Seeger, *Semiconductor Physics* (Springer-Verlag, Berlin and New York, 1985).